

Efficient all-optical quantum computing based on a hybrid approach

Seung-Woo Lee and Hyunseok Jeong
*Center for Macroscopic Quantum Control, Department of Physics and Astronomy,
 Seoul National University, Seoul, 151-742, Korea*

Quantum computers are expected to offer phenomenal increases of computational power [1]. In spite of many proposals based on various physical systems, scalable quantum computation in a fault-tolerant manner is still beyond current technology. Optical models have some prominent advantages such as relatively quick operation time compared to decoherence time [2]. However, massive resource requirements and the gap between the fault tolerance limit and the realistic error rate should be significantly reduced [3]. Here, we develop a novel approach with all-optical hybrid qubits devised to combine advantages of well-known previous approaches. It enables one to efficiently perform universal gate operations in a simple and near-deterministic way using all-optical hybrid entanglement as off-line resources. Remarkably, our approach outperforms the previous ones when considering both the resource requirements and fault tolerance limits. Our work paves an efficient way for the optical realization of scalable quantum computation.

Certain properties of light can be useful to implement qubits, *i.e.*, the basic units for quantum computation [4]. Typically, photons as “particles of light” are considered to encode information with a well-chosen degree of freedom such as horizontal and vertical polarization states, $|H\rangle$ and $|V\rangle$. A major difficulty in this approach is to realize two-qubit gates since photons seldom interact with each other, while single-qubit operations are straightforward [4]. In principle, scalable quantum computation can be achieved without inline non-linear interactions [5], which is often called linear optical quantum computing (LOQC). However, its practical implementation is difficult because fault-tolerant computation requires a very large number of resources [6–8] despite some progress in reducing the scheme-complexity and resource overhead [9–11].

In fact, any two distinct field states in phase space can be explored for a qubit basis [3]. Along this line, the coherent-state quantum computing (CSQC) has been developed with its own merit [12–15]. In CSQC, two coherent states, $|\alpha\rangle$ and $|-\alpha\rangle$ with amplitudes $\pm\alpha$, are used to form a qubit basis and equal superpositions of coherent states, *e.g.*, $|\alpha\rangle+|-\alpha\rangle$ [16], are required as resources [14]. Using this encoding scheme, the Bell-state measurement (B_α in Fig. 1) can be performed in a near-deterministic manner as α gets large [12, 17]. On the other hand, single qubit rotations produce a cumbersome type of errors due

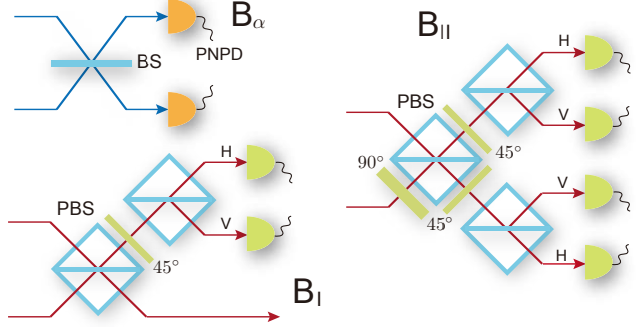


FIG. 1: **Schematics of three Bell-type measurement elements.** A coherent-state Bell measurement, B_α , is implemented by a 50:50 beam splitter (BS) and two photon number parity detectors (PNPD) [12, 17]. B_α unambiguously discriminates between all four Bell states and the success probability is $1 - \exp(-2|\alpha|^2)$. It fails only when no photon is detected at both the detectors. A type-I fusion operation [10], B_I , is implemented by polarizing beam splitters (PBS), wave plates, and photon detectors. It effectively performs $|H\rangle\langle H| |H\rangle\langle H| \pm |V\rangle\langle V| |V\rangle\langle V|$ with a success probability $1/2$ when only one photon is detected at either detectors [10]. A non-deterministic Bell measurement [18] or modified version of the type-II fusion operation, B_{II} , identifies only two of the Bell states, $|H\rangle|V\rangle \pm |V\rangle|H\rangle$, with success probability $1/2$. It succeeds only when one detector from the upper two and another from the lower two click at the same time.

to the non-orthogonality between $|\alpha\rangle$ and $|-\alpha\rangle$ [13, 15], which makes it still difficult to implement deterministic gates [15]. The pros and cons of the two approaches are known: CSQC requires less resources than LOQC but suffers smaller fault-tolerance thresholds [15].

In our approach, the orthonormal basis to define optical hybrid qubits is

$$\{|0_L\rangle = |+\rangle|\alpha\rangle, |1_L\rangle = |-\rangle|-\alpha\rangle\},$$

where $|\pm\rangle = (|H\rangle \pm |V\rangle)/\sqrt{2}$. As we shall see, this approach enables us to overcome particular weak points of both LOQC and CSQC at the same time. The Z -basis measurement can be performed by a single measurement on either of the two physical modes. It can be done on the single-photon mode by a polarization measurement on the basis $|+\rangle$ and $|-\rangle$, or on the coherent-state mode using an ancillary coherent state [13].

In order to construct a universal set of gate operations, Pauli X , arbitrary Z (phase) rotation, Hadamard, and controlled- Z (CZ) gates suffice [1]. The Pauli X

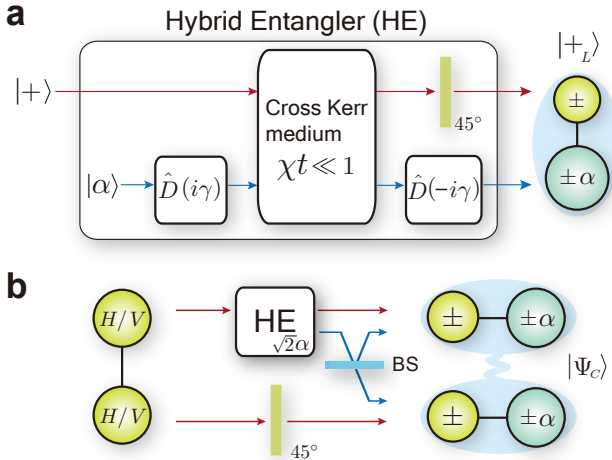


FIG. 2: **Generation of resource entanglement for quantum teleportation.** **a**, Generation of a diagonal state $|+L\rangle \propto |+\rangle|\alpha\rangle + |-\rangle|-\alpha\rangle$ (hybrid pair) using a hybrid entangler (HE) with an arbitrarily weak cross-Kerr nonlinearity. The cross-Kerr nonlinearity with strength χ and interaction time t can induce a transform as $(a|H\rangle + b|V\rangle)|\alpha\rangle \rightarrow a|H\rangle|\alpha\rangle + b|V\rangle|\alpha e^{i\theta}\rangle$ where $\theta = \chi t$ [20]. In a single-photon mode, \pm and H/V denote bases $\{|+\rangle, |-\rangle\}$ and $\{|H\rangle, |V\rangle\}$, respectively. The displacement operator is defined as $\hat{D}(\gamma) = \exp[\gamma\hat{a}^\dagger - \gamma^*\hat{a}]$ where \hat{a}^\dagger (\hat{a}) is the photon creation (annihilation) operator and γ is assumed to be real. **b**, Resource entanglement, $|\Psi_C\rangle$, is generated using a photon pair and a hybrid entangler with simple linear optics elements.

operation (\hat{X}) can be performed by applying a bit flip operation on each of the two modes. The bit flip operation on the single-photon mode, $|+\rangle \leftrightarrow |-\rangle$, is implemented by a polarization rotator, and the operation on the coherent-state mode, $|\alpha\rangle \leftrightarrow |-\alpha\rangle$, by a π phase shifter. An arbitrary Z rotation (\hat{Z}_θ) is performed by applying the phase shift operation only on the single-photon mode: $\{|+\rangle, |-\rangle\} \rightarrow \{|+\rangle, e^{i\theta}|-\rangle\}$, and no operation is required on the coherent-state mode. This is a significant advantage over CSQC in which Z rotations are highly nontrivial and cause a heavy increase of the circuit complexity [15].

A teleportation protocol is necessary to perform near-deterministic Hadamard and CZ operations [19]. An entangled channel, $|\Psi_C\rangle \propto |0_L\rangle|0_L\rangle + |1_L\rangle|1_L\rangle$, for a standard teleportation can be generated using a weak cross-Kerr nonlinear interaction between a two-photon pair, $(|H\rangle|H\rangle + |V\rangle|V\rangle)/\sqrt{2}$, and a strong coherent state together with displacement operations as shown in Fig. 2 [20]. Due to the dual-rail nature of a polarization qubit, an arbitrarily weak nonlinearity together with displacement operations described in Fig. 2a performs a transform as $(a|+\rangle + b|-\rangle)|\alpha\rangle \rightarrow a|+\rangle|\alpha\rangle + b|-\rangle|-\alpha\rangle$, which we shall call a hybrid entangler. In order to generate $|\Psi_C\rangle$, an hybrid entangler should be applied to a two-photon pair with a 50:50 beam splitter and a wave plate

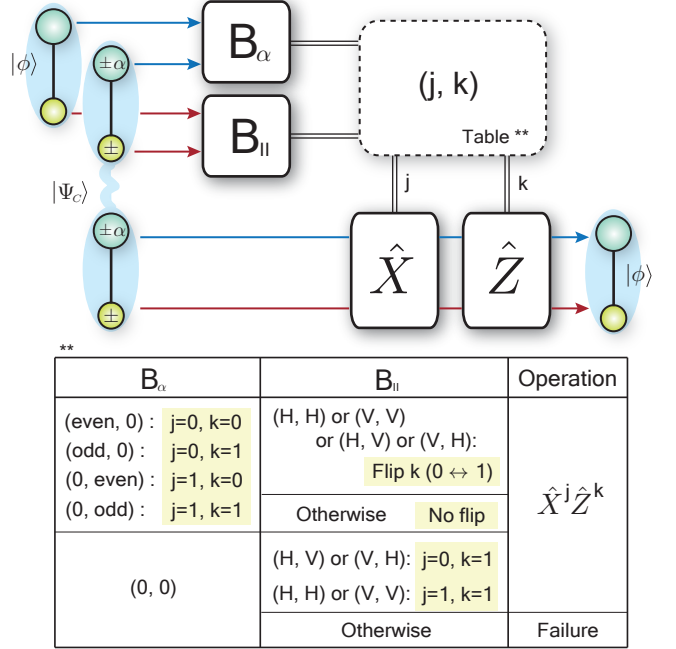


FIG. 3: **Schematic of quantum teleportation for a hybrid qubit.** An unknown hybrid qubit, $|\phi\rangle = a|0_L\rangle + b|1_L\rangle$, is teleported through channel $|\Psi_C\rangle$. B_α and B_{II} are performed on coherent-state modes and photon modes, respectively, between the qubit and one party of the channel state. All possible outcomes and corresponding feed-forward operations are presented in the table. A failure occurs when both B_α and B_{II} fail. The failure probability is found to be $P_f = e^{-2\alpha^2}/2$, and channel $|\Psi_C\rangle$ should be replaced with $|Z\rangle$ ($|Z'\rangle$) in Fig. 4 to perform a Hadamard (CZ) gate.

as shown in Fig. 2b. Two-photon pairs can be obtained using a parametric down converter (PDC) [21].

A key element of the teleportation process is the Bell measurement that discriminates between four entangled states, $|0_L\rangle|0_L\rangle \pm |1_L\rangle|1_L\rangle$ and $|0_L\rangle|1_L\rangle \pm |1_L\rangle|0_L\rangle$. As described in Fig. 3, the Bell measurement for an optical hybrid qubit can be performed using two smaller Bell measurement units, B_α and B_{II} in Fig. 1. Appropriate Pauli operations in the table of Fig. 3 completes the teleportation process with failure probability $P_f = e^{-2\alpha^2}/2$, which outperforms the previous schemes that requires massive overheads with repetitive applications of teleporters [5, 15]. For example, 99% success rate of teleportation is achieved by encoding with $\alpha = 1.4$.

Entangled channels required for Hadamard and CZ gates, $|Z\rangle \propto |0_L\rangle|0_L\rangle + |0_L\rangle|1_L\rangle + |1_L\rangle|0_L\rangle - |1_L\rangle|1_L\rangle$ and $|Z'\rangle \propto |0000\rangle + |0011\rangle + |1100\rangle - |1111\rangle$, where $|0000\rangle = |0_L\rangle|0_L\rangle|0_L\rangle|0_L\rangle$ and so on, can be generated with two-photon pairs and hybrid entanglers as shown in Fig. 4. In order to generate $|Z'\rangle$, either of two nondeterministic methods, G_I or G_α , is employed using B_I or B_α (see Fig. 1), respectively. We emphasize that $|Z\rangle$ and

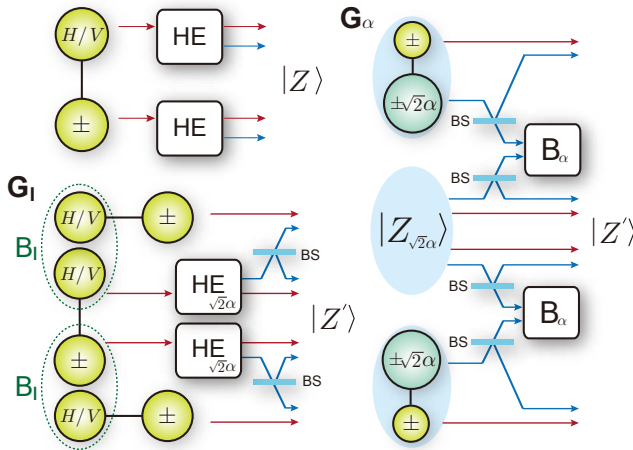


FIG. 4: **Generation methods for resource entanglement required for Hadamard and CZ gates.** State $|Z\rangle$ is generated using one two-photon pair and two hybrid entanglers. State $|H\rangle|+\rangle + |V\rangle|-\rangle$ presented in a graphical representation (top left corner) is obtained by applying a 45 degree wave plate on one mode of a two-photon pair. Two different methods, G_1 and G_α , can be used to generate $|Z'\rangle$. In G_1 , three two-photon pairs and two hybrid entanglers are used with two type-I fusion gates (B_1 in Figure 1) with a final success probability is $1/4$. In G_α , one two-photon pair and four hybrid entanglers together with two B_α measurements with a success probability is $\{1 - \exp(-2|\alpha|^2)\}^2$. Appropriate Pauli rotations for hybrid qubits are required depending on the measurement results of B_1 and B_α .

$|Z'\rangle$ are prepared as off-line resources for gate teleportation [19] while only linear optical elements with photon detections are used for in-line operations.

Errors due to photon losses are considered a major detrimental factor in optical quantum computing [3]. Some errors are immediately noticed during gate operations, which are called locatable errors [3]. Unlocatable errors are detectable only with an error correcting code. Losses at single-photon modes are locatable by B_{II} whenever performing teleportation for Hadamard or CZ gates. Furthermore, a missing photon at a photon mode is immediately compensated in the output qubit $|\phi\rangle$ as far as B_α succeeds as clearly seen in Fig. 3. However, losses at coherent-state modes may cause unlocatable errors besides locatable ones. We analyze each type of Pauli errors caused by photon losses with rate η (see Appendix).

In order to realize scalable quantum computation, the amount of noise per operation should be below a fault tolerant threshold [22–24]. Once a fault tolerant model is determined, the number of resources, required for one round of error correcting may be considered as another crucial factor for scalability. We consider two-photon pairs (*i.e.*, PDCs) and hybrid entanglers (*i.e.*, weak nonlinearities) to be resources. Using the telecorrection protocol [6], noise thresholds and resource requirements in

cluster state LOQC [6, 7], parity state LOQC (pLOQC) [8], and CSQC [15] were previously investigated. Their thresholds and resources are in a trade-off relation, and pLOQC and CSQC have shown the best compromise achievements [3]. In order to compare our approach with previous ones, we follow the same analysis using the 7-qubit STEANE code [25] based on the telecorrection protocol.

The results of our analysis are plotted in Fig. 5 for G_1 and G_α . Remarkably, the threshold level is obviously higher than CSQC for all region of α and is comparable with pLOQC (about 2×10^{-3} [8]), with a greatly reduced cost of resources compared to both CSQC and pLOQC. The threshold peak for each generation scheme appears around $\alpha \approx 1.08$ (Fig. 5a). However, further increase of α lowers the threshold level due to rapid increase of unlocatable errors which are more difficult to correct than locatable ones using the telecorrection protocol [6]. Resource requirements are phenomenally reduced by G_α since the success rate of B_α grows rapidly as α increases. However, the success rate of B_1 is constant ($1/2$) and so are the resource requirements with G_1 . The noise thresholds of G_1 appear to be slightly larger than those of G_α because G_α requires preparation hybrid qubits of amplitudes $\sqrt{2}\alpha$ from the beginning as shown in Fig. 4.

We also note that one can construct a hybrid qubit with an arbitrary number of single-photon modes n . For $n > 1$, the same level of gate success rate is obtained with smaller α than the one required when $n = 1$. Then more errors become detectable using a detection scheme at single-photon modes [11], and the noise threshold raises (but this may consume more resources). Finally, as optical hybrid qubits are interconvertible with photon or coherent-state qubits by inline operations, one can construct hybrid architectures by integrating some devices developed in various approaches, such as quantum memories [26, 27] and photonic chips [28, 29]. Our approach provides an efficient way to implement scalable quantum computation considering resource requirements, fault-tolerance limits and compatibility. An efficient preparation of resource hybrid entanglement [20, 30] would be the next challenge of our scheme.

APPENDIX

Error models. We analyze locatable and unlocatable errors with loss rate η using the master equation $d\rho/dt = \gamma(\hat{J} + \hat{L})\rho$, where $\hat{J}\rho = \sum_i \hat{a}_i \rho \hat{a}_i^\dagger$, $\hat{L}\rho = -\sum_i (\hat{a}_i^\dagger \hat{a}_i \rho + \rho \hat{a}_i^\dagger \hat{a}_i)/2$, and $\hat{a}_i(\hat{a}_i^\dagger)$ is the annihilation (creation) operator for the i -th mode. Here, the loss rate is $\eta = 1 - e^{-\gamma t}$. When the master equation is applied to hybrid qubits, the failure probability P_f for teleportation in Fig. 3 is modified to $P'_f = (1 - \eta) \frac{e^{-2\alpha'^2}}{2} + \eta \frac{2}{1 + e^{2\alpha'^2}}$ where $\alpha' = \sqrt{1 - \eta\alpha}$. If a gate operation fails, the tele-

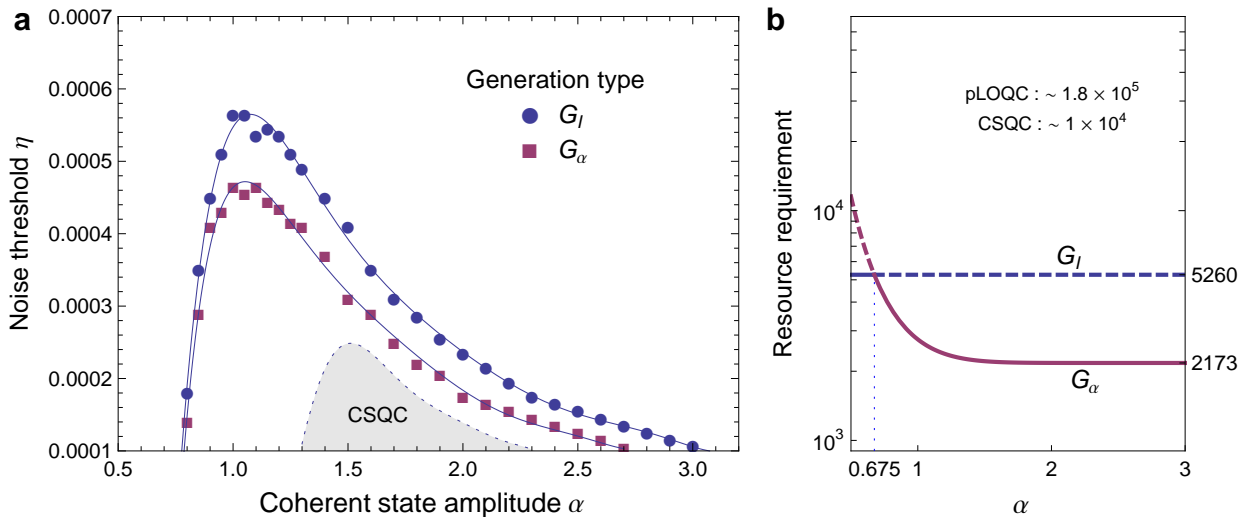


FIG. 5: **Noise thresholds and resource requirements.** **a**, Noise thresholds based on two generation schemes, G_I and G_α , obtained using the 7-qubit STEANE code. **b**, Resource requirements estimated for one round of error correction based on the telecorrection protocol. For G_I , a constant number (5260) of resources (two-photon pairs and hybrid entanglers) are required irrespective of amplitude α , while for G_α the required number of resource states tend to decrease rapidly down to 2173 as increasing α . Two curves intersect at $\alpha \approx 0.675$. We can take the lower curve between them by choosing G_α for $\alpha > 0.675$ and otherwise G_I . It shows a remarkable improvement compared to pLOQC (about 1.8×10^5 [8]) and CSQC (about 10^4 [15]).

ported qubit is assumed to experience depolarization and become fully mixed. This is equivalent to applying a random Pauli operation to the qubit, *i.e.* Z and X Pauli errors occurs independently with the equal probabilities. One can also assume that if a loss occurs in either photon or coherent-state modes, the hybrid qubit experiences a Pauli Z error with probability 1/2. We also model errors due to losses in the generation processes of $|Z\rangle$ and $|Z'\rangle$ as Pauli X and Z errors. We assume that the decrease in amplitude α by loss can be compensated whenever using the teleportation scheme by changing the amplitude of output state of the channel [15]. Based on these models and methods, we have analytically obtained probabilities of aforementioned errors in terms of η .

Error correction. We consider an error correction protocol with several levels of concatenation based on the circuit-based telecorrection [6]. We assume our error model for the lowest level of concatenation. For higher levels, the noise model and error-correction protocol are identical to those of Ref. [6]. We perform a numerical simulation (Monte Carlo method using C++) for one round of the error correction for the first level concatenation. The modified telecorrector circuit is composed of CZ, Hadamard, $|+\rangle$ creation, and X -basis measurement [15].

We carried out a series of simulations for a range of loss rate η and amplitude α . The resulting rates of unlocatable and locatable errors are used for the next level of concatenation for the error correction. If the error rates tend to zero with certain values of η and α in the limit

of many levels of concatenation, fault-tolerant computing is possible with those values. In this way, the noise threshold curves are obtained.

Resource counting. We count the average total number of two-photon pairs and hybrid entanglers for one round of error correction in the lowest level of concatenation. It is assumed [3, 15] that the total number of operations in one round of telecorrection is about 1,000. The fraction of each element used during the telecorrection process can be estimated as [15]: 0.284 (memory), 0.098 (Hadamard), 0.343 (CZ), 0.164 (diagonal state), and 0.111 (X -basis measurement). We also assume parallel productions of resource states and no reuse of resources to avoid using complicated techniques.

- [1] M. A. Nielsen and I. L. Chuang, *Quantum Computation and Quantum Information* (Cambridge Univ. Press, 2000).
- [2] J. L. O'Brien, *Optical Quantum Computing*, *Science* **318**, 1567 (2007).
- [3] T. C. Ralph and G. J. Pryde, *Optical Quantum Computation*, *Progress in Optics* **54**, 209 (2010).
- [4] P. Kok, W. J. Munro, K. Nemoto, T. C. Ralph, J. P. Dowling, and G. J. Milburn, *Linear optical quantum computing with photonic qubits*, *Rev. Mod. Phys.* **79**, 135 (2007).
- [5] E. Knill, R. Laflamme, and G. J. Milburn, *A scheme for efficient quantum computation with linear optics*, *Nature*

409, 46 (2001).

[6] C. M. Dawson, H. L. Haselgrove, and M. A. Nielsen, Noise thresholds for optical cluster-state quantum computation, *Phys. Rev. A* **73**, 052306 (2006).

[7] C. M. Dawson, H. L. Haselgrove, and M. A. Nielsen, Noise Thresholds for Optical Quantum Computers, *Phys. Rev. Lett.* **96**, 020501 (2006).

[8] A. J. F. Hayes, H. L. Haselgrove, A. Gilchrist, and T. C. Ralph, Fault tolerance in parity-state linear optical quantum computing, *Phys. Rev. A* **82**, 022323 (2010).

[9] M. A. Nielsen, Optical Quantum Computation Using Cluster States, *Phys. Rev. Lett.* **93**, 040503 (2004).

[10] D. E. Browne and T. Rudolph, Resource-Efficient Linear Optical Quantum Computation, *Phys. Rev. Lett.* **95**, 010501 (2005).

[11] T. C. Ralph, A. J. F. Hayes, and A. Gilchrist, Loss-Tolerant Optical Qubits, *Phys. Rev. Lett.* **95**, 100501 (2005).

[12] H. Jeong, M. S. Kim, and J. Lee, Quantum-information processing for a coherent superposition state via a mixed entangled coherent channel, *Phys. Rev. A* **64**, 052308 (2001).

[13] H. Jeong and M. S. Kim, Efficient quantum computation using coherent states, *Phys. Rev. A* **65**, 042305 (2002).

[14] T. C. Ralph, A. Gilchrist, G. J. Milburn, W. J. Munro, and S. Glancy, Quantum computation with optical coherent states, *Phys. Rev. A* **68**, 042319 (2003).

[15] A. P. Lund, T. C. Ralph, and H. L. Haselgrove, Fault-Tolerant Linear Optical Quantum Computing with Small-Amplitude Coherent States, *Phys. Rev. Lett.* **100**, 030503 (2008).

[16] A. Ourjoumtsev, H. Jeong, R. Tualle-Brouri and P. Grangier, Generation of optical ‘Schrödinger cats’ from photon number states, *Nature* **448**, 784 (2007).

[17] H. Jeong and M. S. Kim, Purification of entangled coherent states, *Quantum Information and Computation* **2**, 208-221 (2002).

[18] H. Weinfurt, Experimental Bell-State Analysis, *Europhys. Lett.*, **8**, 559 (1994).

[19] D. Gottesman and I. L. Chuang, Demonstrating the viability of universal quantum computation using teleportation and single-qubit operations, *Nature* **402**, 390 (1999).

[20] H. Jeong, Using weak nonlinearity under decoherence for macroscopic-entanglement generation and quantum computation, *Phys. Rev. A* **72**, 034305 (2005).

[21] P. G. Kwiat, K. Mattle, H. Weinfurter, A. Zeilinger, A. Sergienko, and Y. Shih, New High-Intensity Source of Polarization-Entangled Photon Pairs, *Phys. Rev. Lett.* **75**, 4337 (1995).

[22] P. W. Shor, Fault-tolerant quantum computation , in 37th Symposium on Foundations of Computing, IEEE Computer Society Press, Los Alamitos, Ca, pp. 56-65 (1996).

[23] A. M. Steane, Overhead and noise threshold of fault-tolerant quantum error correction, *Phys. Rev. A* **68**, 042322 (2003).

[24] E. Knill, Quantum computing with realistically noisy devices, *Nature* **434**, 39 (2005).

[25] A. M. Steane, Simple quantum error-correcting codes, *Phys. Rev. A* **54**, 4741 (1996).

[26] A. I. Lvovsky, B. C. Sanders, and W. Tittel, Optical quantum memory, *Nature Photonics* **3**, 706 (2009).

[27] H. P. Specht, C. Nolleke, A. Reiserer, M. Uphoff, E. Figueroa, S. Ritter, and G. Rempe, A single-atom quantum memory, *Nature* **473**, 190 (2011).

[28] J. C. F. Matthews, A. Politi, A. Stefanov, and J. L. O’Brien, Manipulation of multiphoton entanglement in waveguide quantum circuits, *Nature Photonics* **3**, 346 (2009).

[29] A. Peruzzo, A. Laing, A. Politi, T. Rudolph and J. L. O’Brien, Multimode quantum interference of photons in multiport integrated devices, *Nature Communications*, **2**, 224 (2011).

[30] B. He, M. Nadeem, and J. A. Bergou, Scheme for generating coherent-state superpositions with realistic cross-Kerr nonlinearity, *Phys. Rev. A* **79**, 035802 (2009).